Calibration and Verification of a MIKE21 Model for Evaluating Shoreline Stabilization Alternatives

Michael B. KABILING, Ph.D., P.E.[1] , Kristen M. ODRONIEC, E.I.[2]

[1]Senior Engineer; Taylor Engineering, Inc., 10151 Deerwood Park Blvd., Bldg. 300, Suite 300, Jacksonville, FL 32256, USA, E-mail mkabiling@taylorengineering.com
[2]Staff Engineer; Taylor Engineering, Inc., E-mail kodroniec@taylorengineering.com

Keywords
MIKE21, 2-D modeling, hydrodynamic, spectral wave, Jupiter Inlet, Florida

Abstract
This study describes the field measurements and numerical modeling of tides and waves south of Jupiter Inlet in Palm Beach County, Florida. As the area suffers from chronic erosion, the ultimate objective of the study is to assess the feasibility of stabilizing the shoreline and develop potential solutions with emphasis on coastal structures. The study includes evaluating historic beach performance, evaluating changes in beach behavior, collecting field data, calibrating and validating a numerical model, and evaluating design alternatives. The present paper summarizes hydrodynamic and wave models calibration and verification. The MIKE21 hydrodynamic (HD) model calibrated and verified well with measured inlet tide levels. The strong influence of the Gulf Stream prevented good velocity calibration. The MIKE21 Spectral Wave (SW) model calibration consisted of fine-tuning the SW module parameters until the model produced a good match between the simulated and measured significant wave heights, peak and mean wave periods, and mean wave directions at the offshore and nearshore measurement stations. Also, test wave model simulations showed little difference in nearshore results between spectral formulation and directionally decoupled parametric formulation at the wave model offshore boundary. Further, the use of directionally decoupled parametric formulation decreased model computational time by 16 times. The study considers the MIKE21 HD and SW models calibrated and verified to apply model tide- and wave-induced currents for the next phase of numerical modeling — sand transport (ST) modeling. The modeling challenge is to simulate long-term shoreline response due to a nearshore structure using the ST model built-in acceleration factor.

INTRODUCTION

The shoreline immediately south of Jupiter Inlet, a stabilized inlet, in Palm Beach County, Florida suffers from chronic erosion. In an effort to assess the feasibility of stabilizing the shoreline, Palm Beach County Department of Environmental Resources Management (ERM) requested that Taylor Engineering develop potential solutions with an emphasis on coastal structures and prepare and submit a Joint Coastal Permit for the proposed solution. The work consists of several phases including evaluating historic beach performance, evaluating changes in beach behavior, collecting field data, calibrating and validating a numerical model, evaluating design alternatives, preparing an environmental assessment, and preparing and submitting a Joint Coastal Permit application. The scope of services also included developing and implementing a plan to concurrently collect wave, current, water surface elevation, and wind data. The data collection supported validation of site-specific hydrodynamic and wave (MIKE21) models. This study summarizes the data collected as per this Florida Department of Environmental Protection approved data collection plan and subsequent model calibration and validation.

FIELD MEASUREMENTS

Inshore Tide Measurements

To evaluate site-specific tidal conditions, Taylor Engineering installed two pressure tide gauges, which collected interior water level measurements near Jupiter Inlet over two, month-long deployment periods. Figure 1 shows one tide gauge (T2) located in the Intracoastal Waterway (ICWW) just north of Jupiter Inlet, and the other tide gauge (T1) located near the mouth of the inlet just inside Dubois Lagoon. The first set of T2 measurements commenced on February 26, 2008 and T2 commenced on April 1, 2008. The removal of both of the interior tide gauges on May 9, 2008 marked the end of the water level data collection for the first set of measurements. The second set of interior water level measurements commenced at both locations on August 15, 2008. On September 6, 2008, an approaching hurricane (Hurricane Ike) prompted the removal of the tide gauge (T1) installed at Dubois Lagoon. Taylor Engineering reinstalled T1 in the same Dubois Lagoon location on September 17, 2008 to continue the interior water level measurements. On September 19, 2008, the removal of both tide gauges marked the completion of the second water level data collection period. Tide range varies from about 1.4 ft (ICWW) to nearly 2.5 ft (Dubois Lagoon) on April 12 – 16, 2008.

Inlet Velocity Measurements

To collect flow velocity data within Jupiter Inlet, this study measured the flow velocity at three locations with a boat-mounted ADCP. The locations consisted of a point near the mouth of the inlet (V1) a point in the ICWW approximately 0.25 mile (mi) north of the inlet (V2), and a second point in the inlet about 0.20 mi west of its intersection with the ICWW (V3). Figure 1 shows the approximate locations of the three velocity measurement stations. The ADCP measured the ebb and flood tidal phases at each of the velocity stations on September 18, 2008, just after retrieval of the ADP's but still within the same hydrological and climatological conditions. Because of unfavorable conditions, no ADCP measurements occurred during the late winter/early spring deployment of the ADP's.

Deployed from a stationary boat, the ADCP recorded the variation of horizontal flow speed and direction along the water depth at Stations V1 – V3 at intervals varying from 1 – 2 hours. Velocity measurements at each station consisted of five-minute recordings of current speed and direction at bins spaced approximately 0.5 m (1.6 ft) along the water depth. The average speed and direction recorded during each measurement provided the depth-averaged flow data at each station.

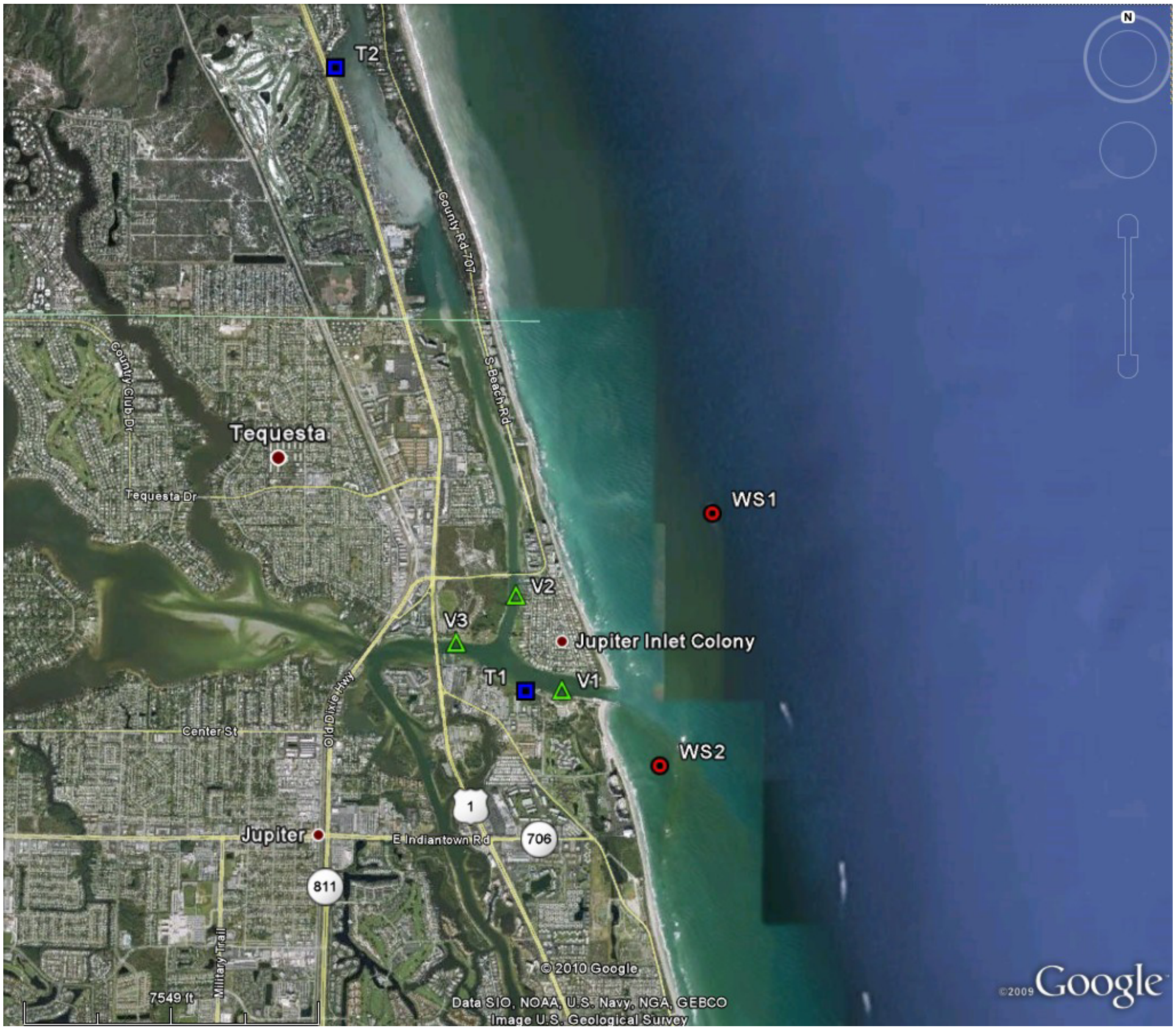

Figure 1: Locations of Tide Gauges (T1, T2), ADCP (V1, V2, V3), and ADP (WS1, WS2) Installations

Figure 2 shows the time series of recorded depth-averaged flow velocity on September 18, 2008 at ADCP stations V1, V2, and V3. The depth-averaged velocity represents the mean of all velocity measurements along the depth at each station. The figure also shows one standard deviation of the velocity measurements for each bin in the water column. At the start of the measurements, the figure shows flood velocities flowing westerly through Jupiter Inlet (V1 and V3) and northerly through the ICWW (V2). By 11:00 a.m., the northerly flow at V2 reversed (flowed southerly). At stations V1 and V3, the westerly flow started to weaken after the initial measurements. Several hours later (12:30 p.m. at V1 and 1:20 p.m. at V3), both stations reversed flow eastward when ebb tide occurred. The neighboring inlet to the north, St. Lucie Inlet, likely dominated the flow at V2 during portions of these tidal velocity measurements.

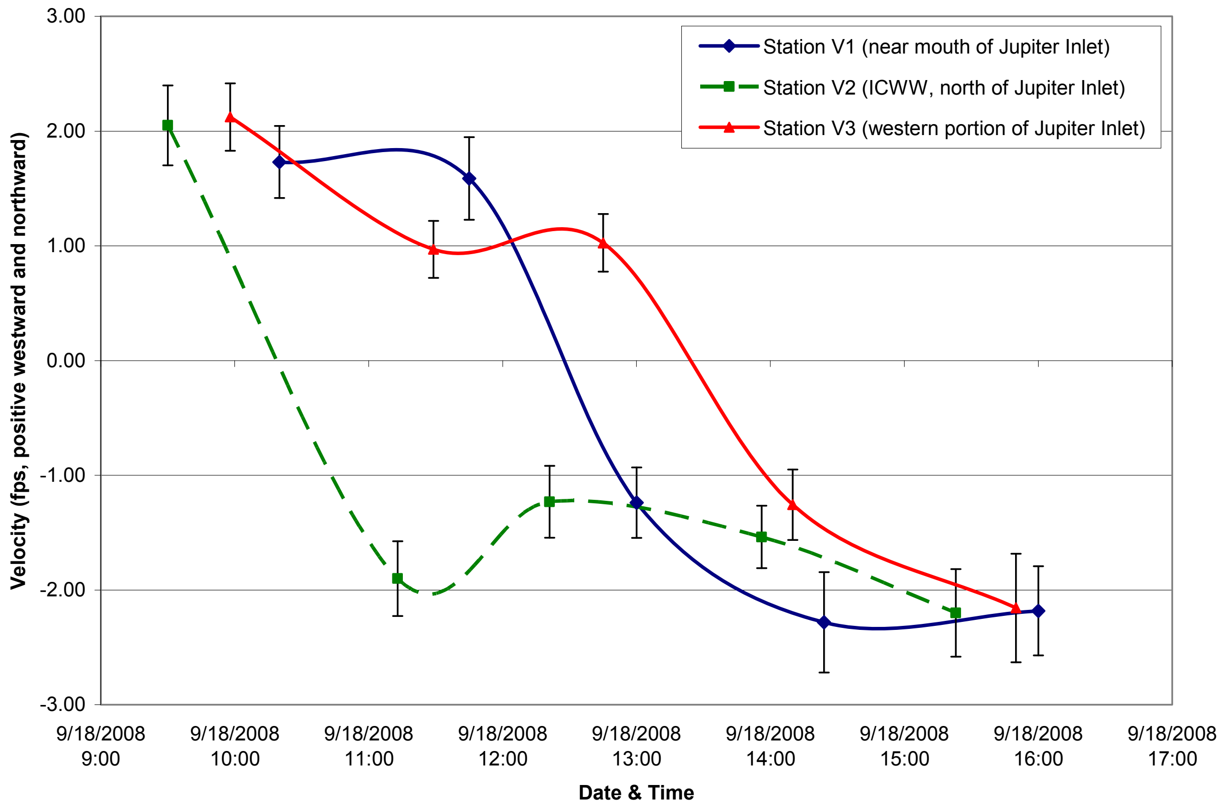

Figure 2: Measured Flow Velocity at V1, V2, and V3 (September 18, 2008)

Nearshore and Offshore Measurements

A subcontractor, Scientific Environmental Applications, Inc. (SEA) measured offshore and nearshore water level, flow velocity, and wave data using two ADP's — one just southeast of Jupiter Inlet inside the ebb shoal (WS2) and the other northeast of Jupiter Inlet in approximately 10 m (30 ft) of water (WS1). The first and second collections of measurements occurred March 29 – May 5, 2008 and August 14 – September 6, 2008. In addition to normal periods, the instruments also measured wave and wind conditions during two storms: Tropical Storm Fay (near August 20) and another over the period August 30 – September 6 as Hurricane Ike approached Florida. SEA retrieved the ADP's on September 6 earlier than scheduled because of fear of losing the instruments to an approaching hurricane (Hurricane Ike). The ADP's collected data as a time series of water depths, flow velocities, and wave measurements. The recorded water depths referred to the distance from the top of each of the ADP sensors to the water surface. The ADP's recorded flow velocities — including current speed and direction — in each of five vertical bins across the water column. The wave measurements consisted of significant wave height, mean and peak wave period, and mean and peak wave direction.

SEA surveyed the elevation of the top of the sensor at WS2 before and after each deployment so that the water levels could reference a datum. A surveyor looking from the beach to a survey rod held on top of the ADP by a diver and a person on the boat determined the elevation of the instrument's transducer. (Note that a surveyor proved unavailable during the September instrument retrieval.) This procedure helped determine the portion of measured water level rise attributable to sinking or settling of the instrument.

Currents at WS1 flow mainly in a northwesterly direction and occasionally in a northeasterly direction and the waves generally originate from the east and northeast. This study postulates that this gauge, in 10 m (30 ft) of water, may have recorded the influence of the Gulf Stream, which approaches relatively near the Florida coast in this area. Satellite thermal images of the western wall of the Gulf Stream and its fluctuations during the data collection periods appear to support this hypothesis.

Figures 3 and 4 show the wave and current directions measured during both data collection periods as well as the significant wave heights measured offshore at WS1. As seen in these figures, WS1 and WS2 currents tended to flow in a northwesterly direction and occasionally in a northeasterly direction during periods with normal wave activity. However, during periods with large waves, such as nor'easters (during the first data collection period) and tropical storms (during the second data collection period), waves appear to exert more influence on current direction — especially during the first data collection period when waves approach from a direction less consistent with the northward influence of the Gulf Stream. For example, waves originate from the east-northeast during the period April 15 – 19 in Figure 3. If Gulf Stream influence is strong, measured current directions should flow northwesterly (340 degrees) during that period. Instead, measured currents (possibly caused by eddies) flowed southeasterly (160 degrees). In Figure 4, waves generally originate from the east-southeast (100 degrees) and measured currents flowed toward the northwest (340 degrees) (originating from a southeasterly direction). As shown in Figure 4, waves traveling in a similar direction to the Gulf Stream appeared to have a lesser effect on measured current direction.

Wind Data

In keeping with the FDEP-approved data collection plan, Taylor Engineering gathered wind data from the National Data Buoy Center C-MAN Lake Worth Station LKWF1 (located 22.7 mi south of the study area at 26°36′42″N, 80°02′00″W) to characterize the wind conditions during each of the data collection periods. Knowledge of the wind climate can provide an understanding of wave growth from wind as well as the affect of wind on currents. The wind speed and wind direction during the first data collection period (March 29 to May 5, 2008) averaged 4.1 m/s. The wind speed and direction during the second data collection period (August 14 to September 6, 2008) averaged 4.0 m/s.

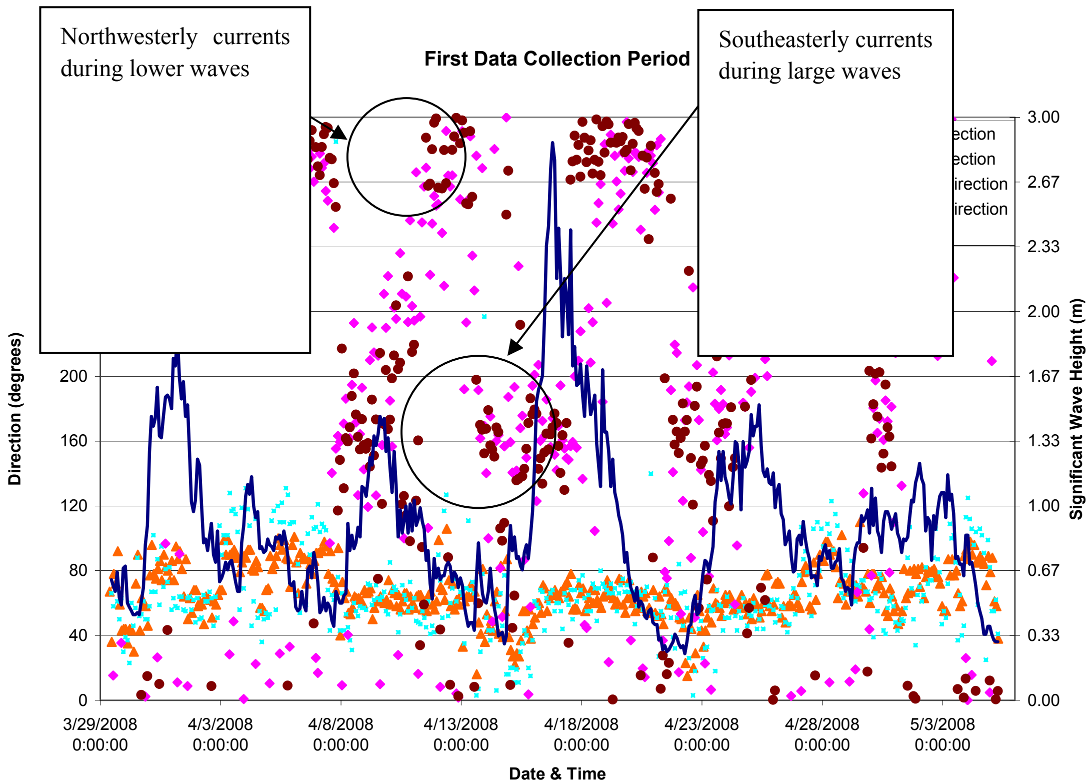

Figure 3: Current and Wave Directions Measured at WS1 and WS2 during First Data Collection Period (March 29 – May 5, 2008)

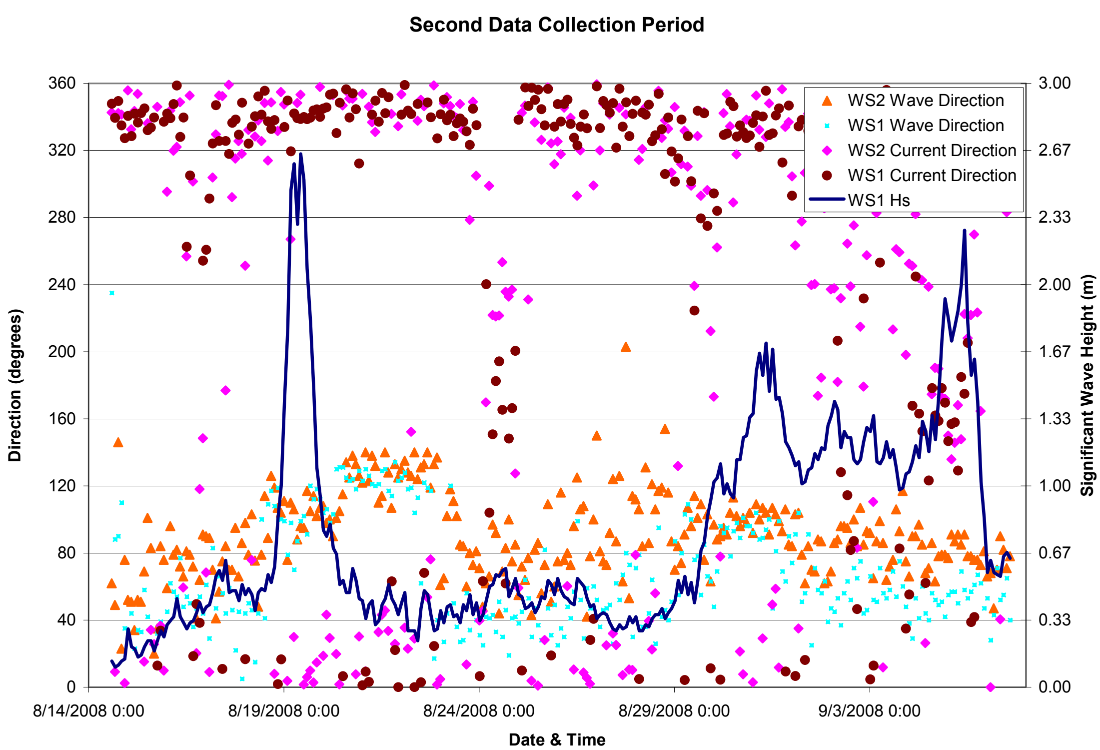

Figure 4: Current and Wave Directions Measured at WS1 and WS2 during Second Data Collection Period (August 14 – September 6, 2008)

NUMERICAL MODELING

Model Mesh

Mesh development for this study takes advantage of several existing model meshes originally generated for the Jupiter Inlet and Lake Worth Inlet areas. Taylor Engineering generated the MIKE21 FM model mesh from the these model meshes and limited the MIKE21 FM mesh to approximately 40.5 kilometers (km) (25.2 mi) north of Jupiter Inlet (north ocean boundary), 25.5 km (15.8 mi) east of Jupiter Inlet (offshore boundary), 46.3 km (28.8 mi) south of Jupiter Inlet (south ocean boundary), and 4.8 km (3.0 mi) north of the Intracoastal Waterway's (ICWW) intersection with Jupiter Inlet (ICWW north boundary). Availability of wave information (U.S. Army Corps of Engineers' Wave Information Study) and NOAA tide predictions and consideration of possible wave directions guided the selection of model boundary locations. At the area of interest just offshore the shoreline south of Jupiter Inlet, small elements provided the means to evaluate in more detail the hydraulic and wave conditions at the site.

To construct the mesh, multiple sources provided the bathymetric data — NOAA nautical charts, Palm Beach County 2006 beach survey, Jupiter Inlet November 2007 ebb shoal survey, ICWW October 2005 and June 2007 surveys, Jupiter Inlet 2007 sand trap survey, Martin County beach survey, and elevation data from previous hydraulic models. Figure 5 shows the model domain bathymetry referenced to North American Vertical Datum of 1988 (NAVD). Red indicates areas above 0.0 meters-NAVD (m-NAVD). The right-hand portion of Figure 5 contains a detailed image of the model mesh near the study area (green box). The fine mesh resolution in the detailed image defines the potential location of shoreline protection structure. The mesh horizontal control references the UTM North American Datum of 1983 (NAD83) Zone 17.

Model Boundary Conditions

The hydrodynamic module contains two time-varying elevation boundary conditions — one at the offshore model boundary and the other at the north ICWW boundary. The spectral wave module applied one time-varying wave parameter boundary condition at the offshore model boundary. Because of proximity to the model's offshore boundary, the measurements at WS1 provided the model's offshore boundary conditions. Measured water levels and wave parameters (height, period, and direction) collected at WS1 on March 29 – May 5, 2008 provided the water level and wave parameter forcing data at the offshore model boundary for the model calibration. Measured water levels collected by a tide gauge in the ICWW just north of Jupiter Inlet (T2) on February 26 – May 9, 2008 provided the water level forcing data at the northern ICWW model boundary during model calibration. Similarly, during model verification, measured water levels and wave parameters (including height, period, and direction) collected by WS1 on August 14 – September 6, 2008 provided the water level and wave parameter forcing data at the offshore model boundary. In addition, measured water levels collected by T2 on August 15 – September 19, 2008 provided the water level forcing data at the ICWW north model boundary for the model verification. Figure 1 shows these measurement locations relative to each other.

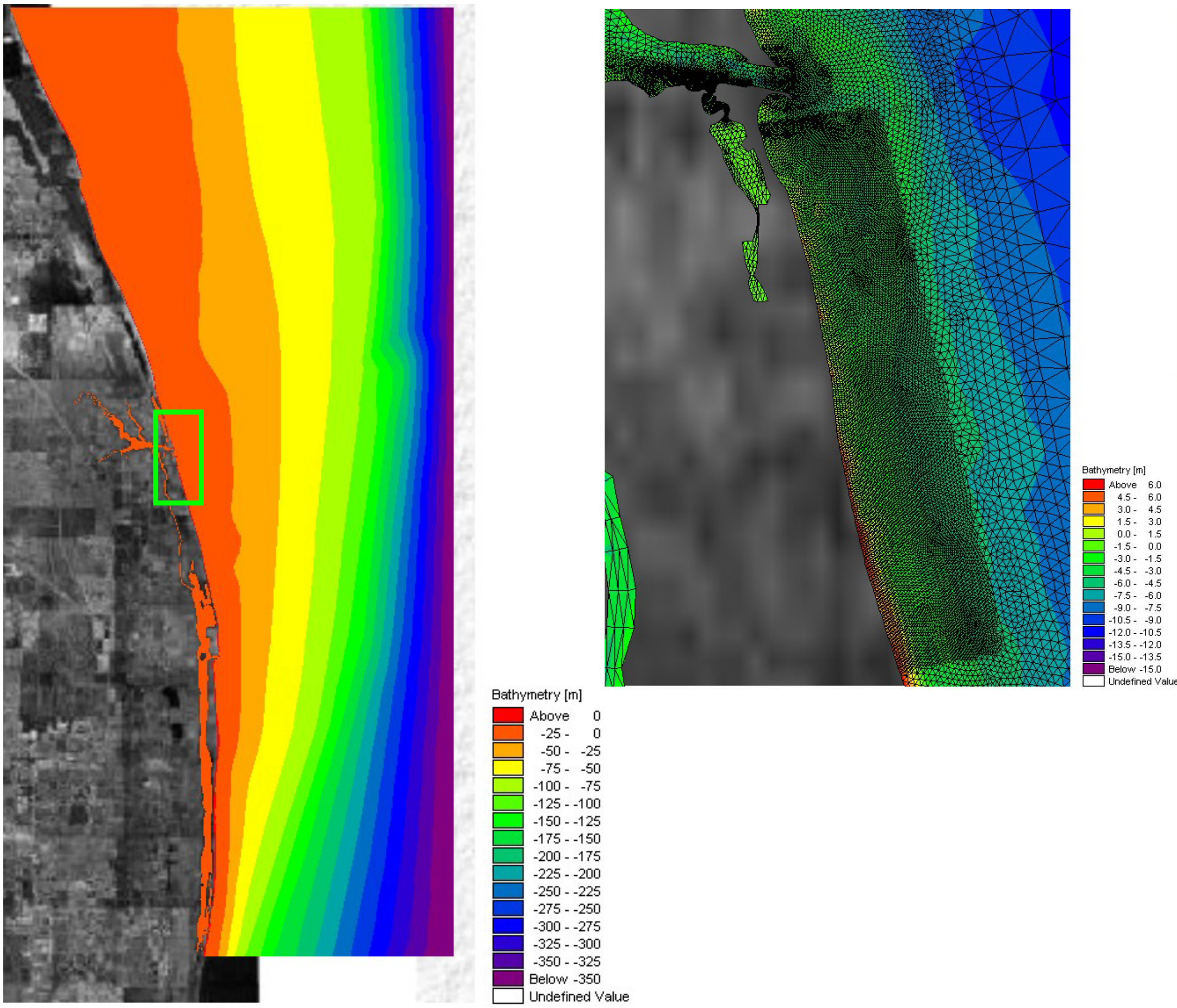

Figure 5: MIKE21 Model Domain

<u>Model Calibration</u>

Calibration consisted of iterative adjustments to model parameters until the model results agreed with the measured data. Taylor Engineering applied the model parameters as adjusted in model calibration to model verification and in normal tide model simulations. The measured data available for calibration consisted of water level measurements at four locations — two interior locations (T1 and T2) and two offshore locations (WS1 and WS2) — and flow and wave measurements at the same two offshore locations (WS1 and WS2).

Water Level Calibration

Calibration consisted of producing water levels consistent, first with data at WS2 and second with data at T1. March and May 2008 T2 and WS1 water level data provided the model boundary uniform water level conditions at the ICWW north and offshore boundaries. The calibrated HD model parameters included a Manning's *n* of 0.02 for all open ocean areas and 0.03 to 0.035 for all estuary, river, and ICWW areas; a Smagorinsky formulation of 0.5; and a CFL number of 0.8. The values chosen for the Smagorinsky formulation; the CFL number; and the Manning's *n* for the estuary, river, and ICWW areas fall within the ranges recommended in the DHI users' manual.

Figure 6 shows a comparison of the measured and model-simulated water surface elevations at WS2 over a calibration period of approximately 24 days. Except for a slight overestimation of high and low tides near the end of the calibration period, this figure shows good agreement between data and model-simulated water elevations. Although the model tended to slightly underestimate high and low tides during approximately the first 14 days of the calibration period and to slightly overestimate them during the last 10 days (likely due to instrument settlement), this figure also shows generally good agreement between the data and simulated water surface elevations. The computed water surface elevations deviate from the 24-day long, 2-hour data set an average 0.03 m (0.1 ft or 5% of mean tidal range) at WS2 and an average 0.07 m (0.2 ft or 9% of mean tidal range) at T1.

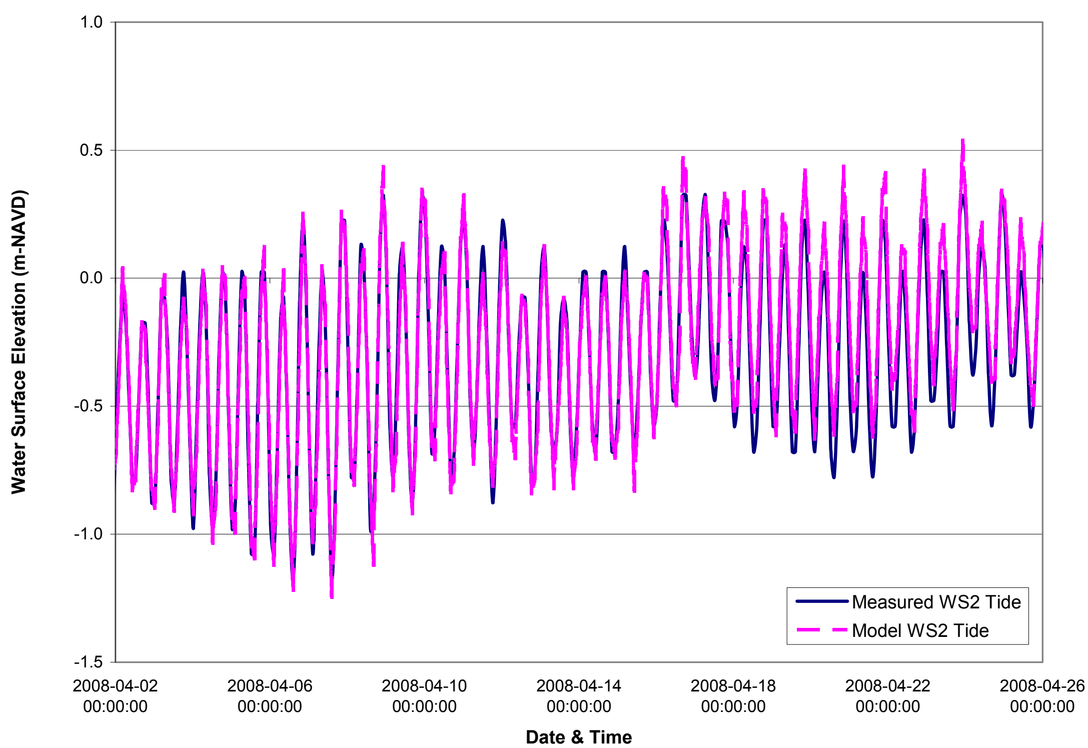

Figure 6: Comparison of Simulated and Measured Water Surface Elevations at WS2 during Calibration

Flow Velocity Calibration

The authors believe (and model test simulations show) that winds did not contribute significantly to the measured currents because the wind data showed low wind speeds over the calibration period. Therefore, the present study limited the flow calibration to tide- and wave-generated current related parameters. However, adjustment of wave forcing parameters could not produce a good match between the simulated current magnitudes and directions and the measured current magnitudes and directions. As an example, because measured wave data during the calibration period generally reflects northeast waves, the model produced consistent currents flowing from a similar direction. However, as Figure 7 shows, the measured currents showed a general trend of flowing northwest (330 degrees from north) (and occasionally northeast [30 degrees from north]). The difficulty in calibrating the flow may result from the northern influence of the Gulf Stream on the measured currents in the study area. The measured currents at both locations tended to flow north. This tendency suggests strong influences from the Gulf Stream at the offshore ADP (WS1) and a slightly less consistent, but nonetheless apparent, Gulf Stream influence at the nearshore ADP (WS2). Because the measured waves at the same locations during the same period originate from the northeast, the currents would unlikely flow so consistently northwest and northeast unless the Gulf Stream somehow affected the measurements.

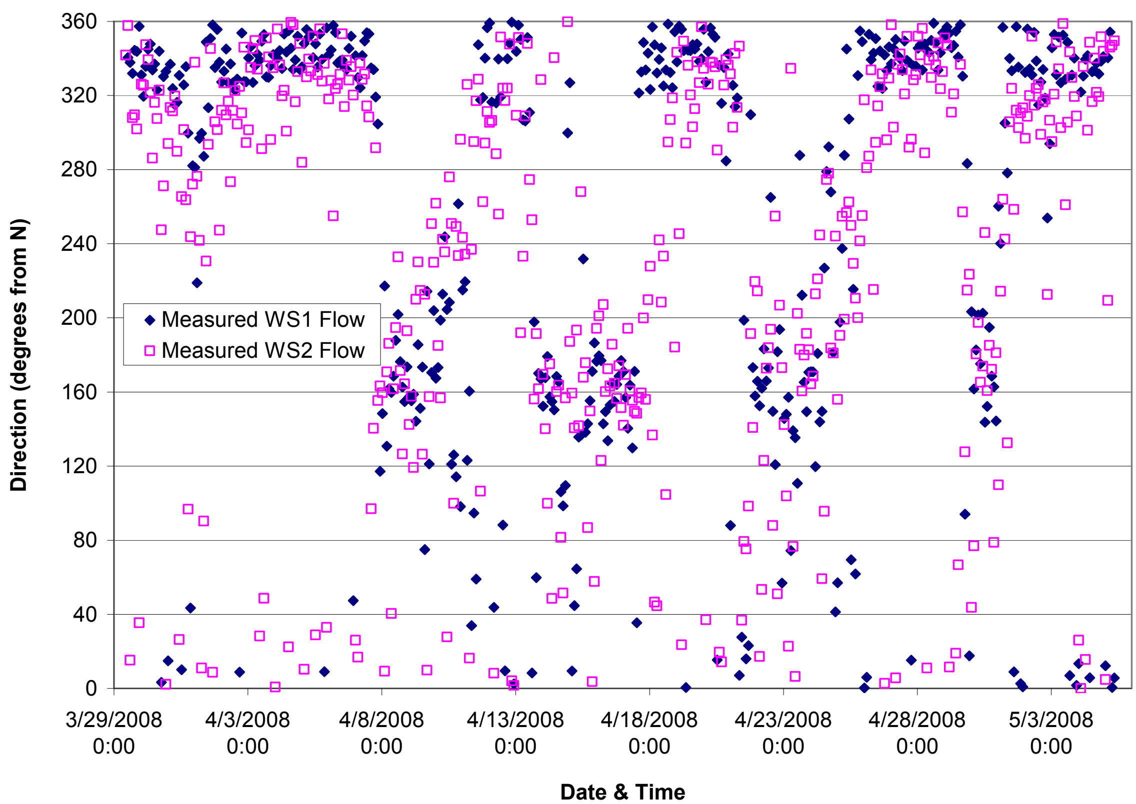

Figure 7: Measured Current Directions at WS1 and WS2

This study attempted to incorporate the effects of the Gulf Stream by introducing two additional boundary conditions — one at the southern limit of the model domain and the other at the northern limit. These boundary conditions introduced a northward flow entering the model domain at the southern limit and an equal flow exiting at the northern limit. The assumed northward direction of the Gulf Stream and measured velocity data at WS1 and WS2 provided rough estimates of the northward flow magnitude and direction. Variations of these boundary conditions produced slightly different model flow results at the offshore (WS1) and nearshore (WS2) locations. In general, the results at WS1 matched the flow measurements more closely than the runs without flow inputs at the south and north boundaries. At the nearshore area, a comparison of results from the model simulations including the Gulf Stream effect with those from simulations that excluded the effect show a worse match with the nearshore flow measurements.

These contrasting observations — an improved match offshore and a worse match nearshore — are consistent with a Gulf Stream that drifts in and out of the nearshore area. This east-west lateral movement of the Gulf Stream can potentially generate local eddies and consequently result in measured net flows whose magnitude and direction appear opposite or inconsistent with the tide- and wave-generated currents. Because the nearshore ADP (WS2) located approximately 305 m (1,000 ft) from the coastline, its measured data likely reflects local eddies. Located just over 1.6 km (nearly a mile) from the shoreline, the offshore ADP (WS1) likely measured a more stable (in magnitude and direction) portion of the Gulf Stream. Notably, the Palm Beach County, Florida Shore Protection Project General Design Memorandum (1994) confirms this assumption by defining the location of the Gulf Stream (or Florida Current) as approximately one mile offshore of the shoreline in this area. This hypothesis supports the general improvement in model results offshore and the worsening of the results nearshore when the model simulations included the effect of the Gulf Stream.

To improve model results nearshore, one must supply the temporal and spatial variation of the Gulf Stream at the model's north and south boundaries. Unfortunately, because the model domain comprises only a very small portion of the area influenced by the Gulf Stream, the effect of the Gulf Stream proves difficult to quantify near the study area. Existing regional models that show Gulf Stream movement with time likely contain large element sizes too coarse to provide appropriate resolution at the south and north boundaries of the MIKE21 Coupled Model FM. Further, as shown by the current directions plotted in Figures 8 and 9, during periods of high waves (e.g., April 15 – 19 when littoral transport is large), the effect of the Gulf Stream likely weakens when compared to wave-generated currents. The observed alongshore sedimentation pattern updrift and downdrift of the area of interest supports this hypothesis (i.e., a southward net littoral transport). If the Gulf Stream consistently exerts a greater influence than waves at the area of interest, then the sediment pattern would have indicated a northward or greatly reduced southward net littoral transport. Because available sedimentation data (e.g., sediment budgets, beach surveys, etc.) at the area support a southward net littoral transport, the MIKE21 Coupled Model FM need not include the Gulf Stream effects to analyze the effects of nearshore coastal processes.

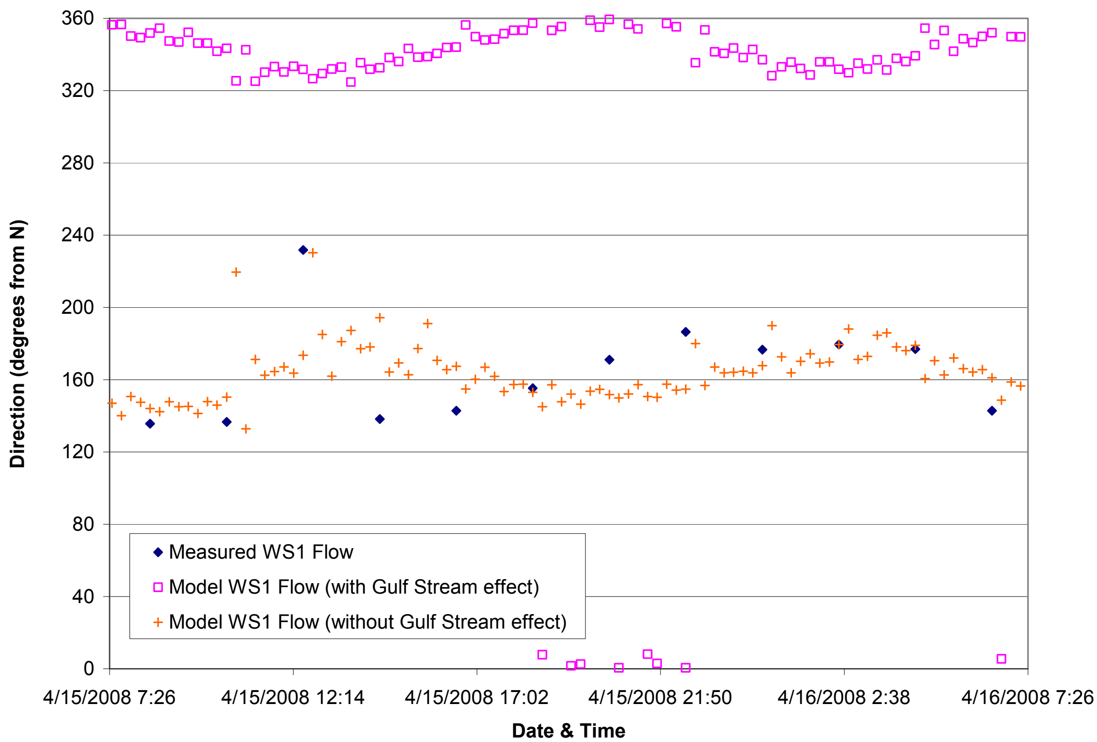

Figure 8: Comparison of Measured and Simulated Current Flow Directions during Large Wave Event at WS1

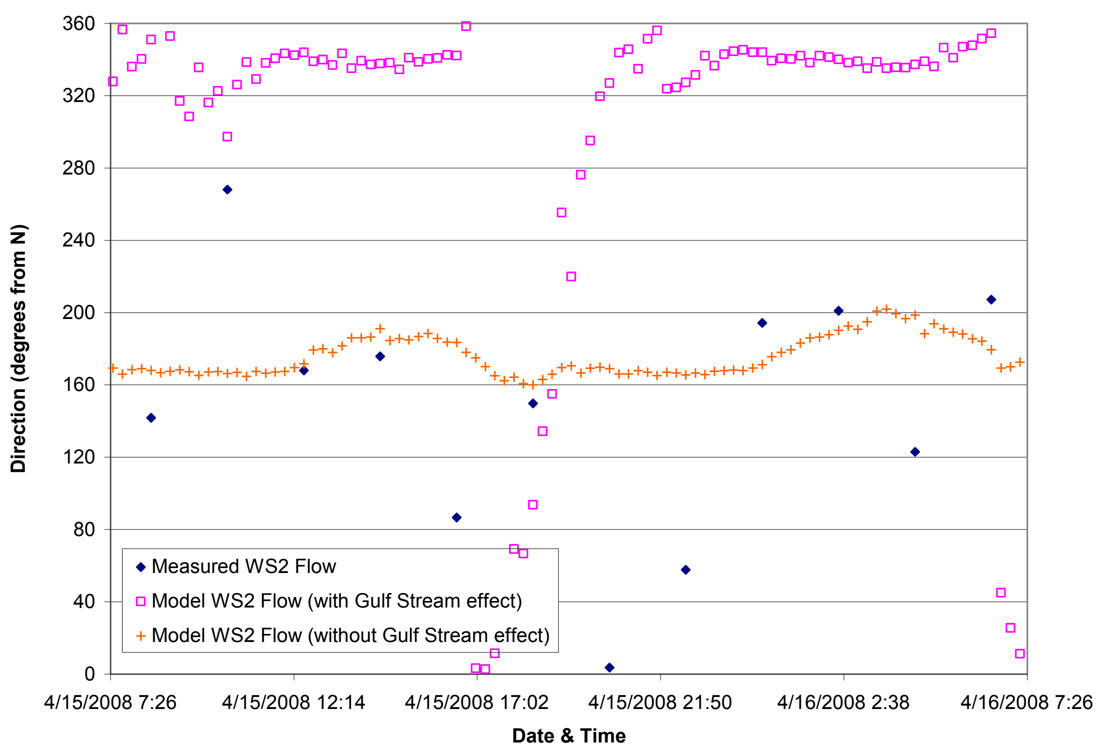

Figure 9: Comparison of Measured and Simulated Current Flow Directions during Large Wave Event at WS2

Wave Calibration

Wave calibration consisted of fine-tuning SW module parameters so that the model produced a good match between the simulated and measured significant wave heights, peak and mean wave periods, and mean wave directions at the offshore (WS1) and nearshore (WS2) locations. This study applied non-breaking wave data to calibrate the SW wave module because wave models (such as MIKE21) do not provide good estimates of waves in the surf zone. Thus, this study applied WS1 wave data measured at the offshore boundary and compared model and measured wave properties at WS2. WS2 breaking wave data provided the means to simulate the location of wave breaking. The following paragraphs provide a detailed description of the wave module calibration and testing.

Offshore forcing wave data for the wave module calibration included wave parameters at the offshore boundary — consisting of measured significant wave heights, peak wave periods, and mean wave directions at WS1 — and zero waves at the other model boundaries. The dynamic link between the wave and hydrodynamic modules automatically incorporates the effect of tides on wave propagation.

Comparisons of nearshore results between spectral and directionally decoupled parametric formulations at the wave model offshore boundary showed little difference. However, model runs were approximately 16 times faster in decoupled parametric formulation than in the fully spectral mode. Parameters that can influence wave calibration in the SW module with directionally decoupled parametric formulation include bottom friction, breaking parameters, current and water level data, and boundary data. The only boundary data included in the SW module consisted of wave parameters varying in time and spatially uniform along the ocean boundary. The boundary types for the other model boundaries consisted of a closed boundary at the northern ICWW boundary. The current and water level data consisted of results from the HD module that ran concurrently with the SW module. The only two remaining factors for parameter adjustment that could influence wave calibration consisted of the bottom friction and wave breaking parameters.

Among the parameter options available for including wave breaking in the model, the specified breaking index (g) equal to a constant 0.4 provided the best simulated wave parameter match with the measured data. Note that for this study, the only reason to calibrate the wave breaking parameters is to establish the location of wave breaking. Finally, of the four possible bottom friction models, the DHI users' manual recommends the default Nikuradse roughness model. Notably, the manual suggests multiplying the local median grain size D_{50} by two to get an appropriate estimate of the roughness parameter (k_N) in a sandy area. The users' manual also states that the presence of bed forms or ripples could necessitate a much larger k_N value. Execution of several sensitivity runs provided information on the influence of various bottom friction values. Comparison of the sensitivity runs with the measured wave data indicated the most appropriate values to apply for the study area. Based on the sensitivity run results and comparison to the measured data, application of a roughness parameter of 0.34 mm (approximate D_{50} value) offshore and 1.02 mm (three times D_{50}) nearshore resulted in the best wave calibration at WS1 and WS2.

Figures 10 and 11 show the comparisons of measured and simulated wave parameters at WS1 and WS2 over a nine day calibration period. In each figure, the top graphs show the significant wave heights and wave directions, and the bottom graphs show the peak and mean wave periods. Figure 10 exhibits excellent agreement between data and simulated wave heights, directions, and peak wave periods. On April 16 – 19, Figure 11 displays a case where high wave heights and shallow bathymetry caused waves to break before reaching WS2. Apart from this discrepancy, the figure also shows generally good agreement between the data and the simulated wave parameters.

Figures 10 and 11 also show some variation between the measured and simulated mean wave periods. These variations result from the fact that, while running in the directionally decoupled wave propagation mode, the wave model assumes a constant wave spectrum shape. As such, the model calculated mean wave periods equal a nearly constant factor of the peak wave periods. (Note that in Figures 10 and 11 the modeled mean wave periods mimic the same shape as the modeled peak wave periods.) Compared to swell conditions, wind-generated waves effectively lower mean wave periods by introducing high frequency wave energy. Because the measured wave data include the effects of wind (not modeled in the study simulations), lower mean wave periods result in the measured data when compared to the modeled mean wave periods.

Field Measurement Uncertainty

As the slight discrepancies in Figures 10 and 11 show, limitations, or uncertainties, exist in wave simulation models and measurements that can prevent an exact match between simulated and measured wave heights, periods, and directions. This derives from uncertainties within the actual measured data as well as uncertainties in the simulation results. Because of these uncertainties, one must acknowledge that a range exists within which the measured wave parameters and the simulated wave parameters can occur. Kamphuis (2000) provides a discussion of uncertainty in wave measurements and modeling. Kamphuis defines uncertainty as quantifying "the combination of errors, randomness and general lack of physical understanding." The following equation gives the definition of uncertainty, or "coefficient of variation:"

$$\sigma'_H = \sigma_H / H_{mean} \qquad (1)$$

where σ'_H represents uncertainty in wave height, σ_H represents the standard deviation (or "error") of wave height, and H_{mean} represents the mean wave height value.

From the definition of standard deviation, wave parameters occur within one standard deviation of the average wave parameter 68% of the time, within two standard deviations 95% of the time, and within three standard deviations almost all of the time. Calculation of the standard deviation derives from reasonable uncertainty values. Kamphuis defines ranges of reasonable uncertainty values (σ'_H) as 0.05 to 0.15 for measured wave heights, 0.2 to 0.4 for wave directions, and 0.05 to 0.2 for wave periods. As seen in the equation defining uncertainty, as a wave height increases, so does its error (σ_H). The same remains true for other wave parameters. Therefore, errors increase with greater parameter magnitude and decrease with lesser parameter magnitude. Note that simulated wave parameters produce even higher levels of uncertainty than measured wave parameters. Kamphuis considers 0.25 to 0.3 as a reasonable uncertainty range for simulated wave heights and periods; simulated wave directions have even higher uncertainty.

In conclusion, despite some discrepancies between the measured data and the simulation results, the applied model produces very reasonable estimates in light of the large uncertainties inherent in both measured and simulated wave parameters.

Model Validation and Verification

The first step to determine the accuracy of the model consisted of confirming that the wave calibration data proved analytically sound. A Coastal Engineering Design & Analysis System (CEDAS) program called NEMOS (Nearshore Evolution Modeling System) executed this analytic validation of the data. One of the utilities within NEMOS — WISPH3 — transforms waves from a deeper water depth to an arbitrary shallower water depth based on user-defined wave heights, periods, and directions and an assumption of straight and parallel contours. For this study, WISPH3 transformed the wave parameters measured offshore at WS1 to a depth consistent with that of WS2 — approximately five meters (16 ft). This procedure ensured consistency of measured wave data between WS1 and WS2.

Figures 12, 13, and 14 show the WISPH3-transformed wave parameters compared to the measured data at WS2. During normal wave conditions, the WISPH3-transformed wave heights match the measured WS2 data closely. However, during high waves, such as the nor'easter that occurred on April 16 – 19, 2008, WISPH3 overestimated the wave heights. This overestimation likely results from the fact that the measured data reflects waves breaking — because of the shallower depths surrounding WS2 — before reaching WS2. Because WISPH3 transforms waves based on only two user-defined depths, and not on all surrounding bathymetry, it cannot account for these shallower depths offshore of WS2. Consequently, the results cannot reflect the prior wave breaking. For the same reason, WISPH3 could not produce wave directions similar to the measured directions. Additionally, the measured wave periods' oscillation between high and low period (swell vs. sea) waves indicate dual-peak spectra. The differences between the measured wave periods and WISPH3 wave periods result from the fact that WISPH3 performs a simplified wave transformation and consequently cannot reproduce these highly variable wave periods.

The next and final step included ensuring that the parameters applied to achieve good model performance during the calibration period also apply to simulations outside the calibration period. To verify the performance of the model, this study updated the model's boundary conditions to include forcing data (measured water levels at T2 and WS1 and wave parameters at WS1) covering a week-long period from August 18 – 24, 2008, and compared the model's simulated tide levels and wave parameters with the measured tide levels at WS2 and with the measured wave parameters at WS1 and WS2.

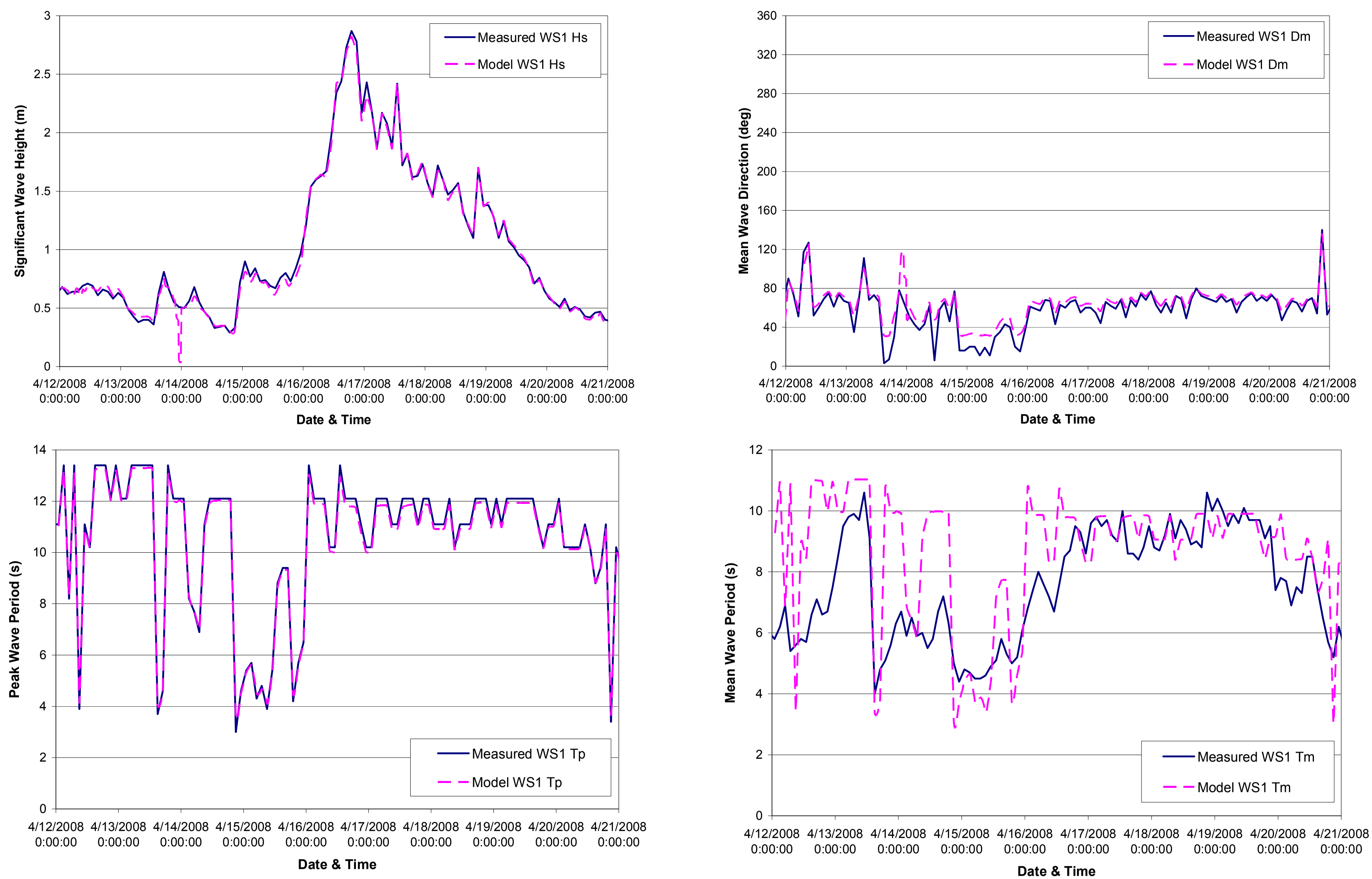

Figure 10: Comparison of Measured and Simulated Wave Parameters April 12 – 21, 2008 at WS1

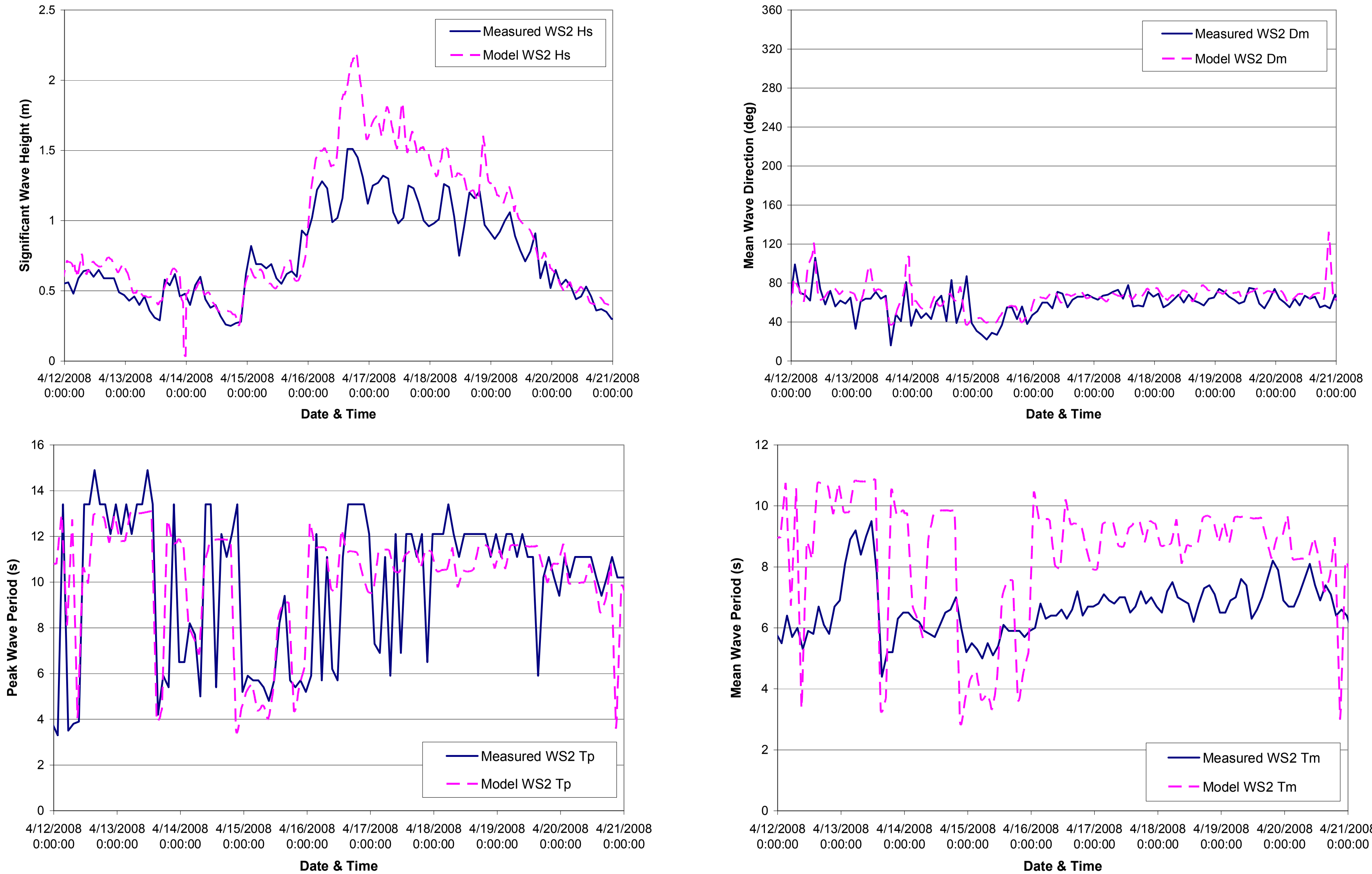

Figure 11: Comparison of Measured and Simulated Wave Parameters April 12 – 21, 2008 at WS2

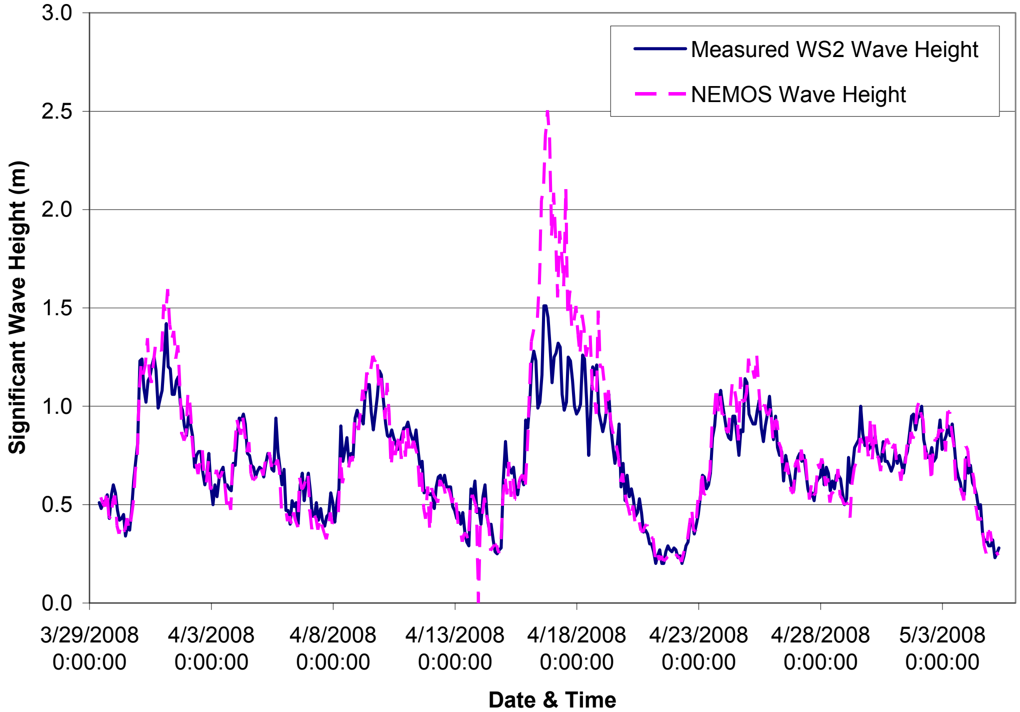

Figure 12: Comparison of Measured Wave Heights with WISPH3-Transformed Wave Heights at WS2

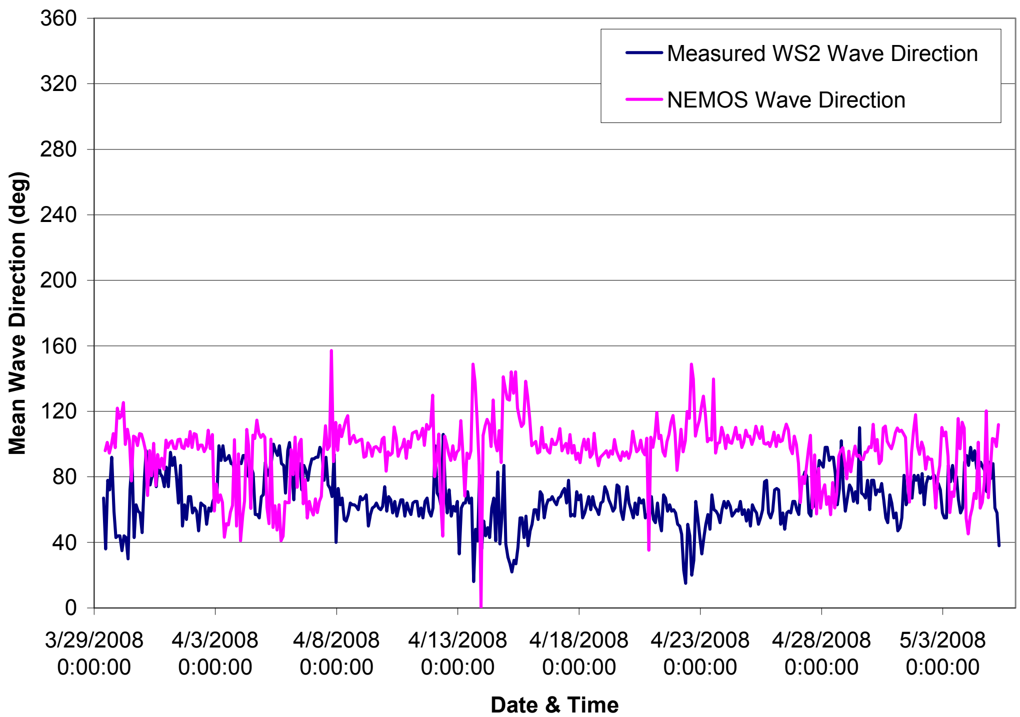

Figure 13: Comparison of Measured Wave Directions with WISPH3-Transformed Wave Directions at WS2

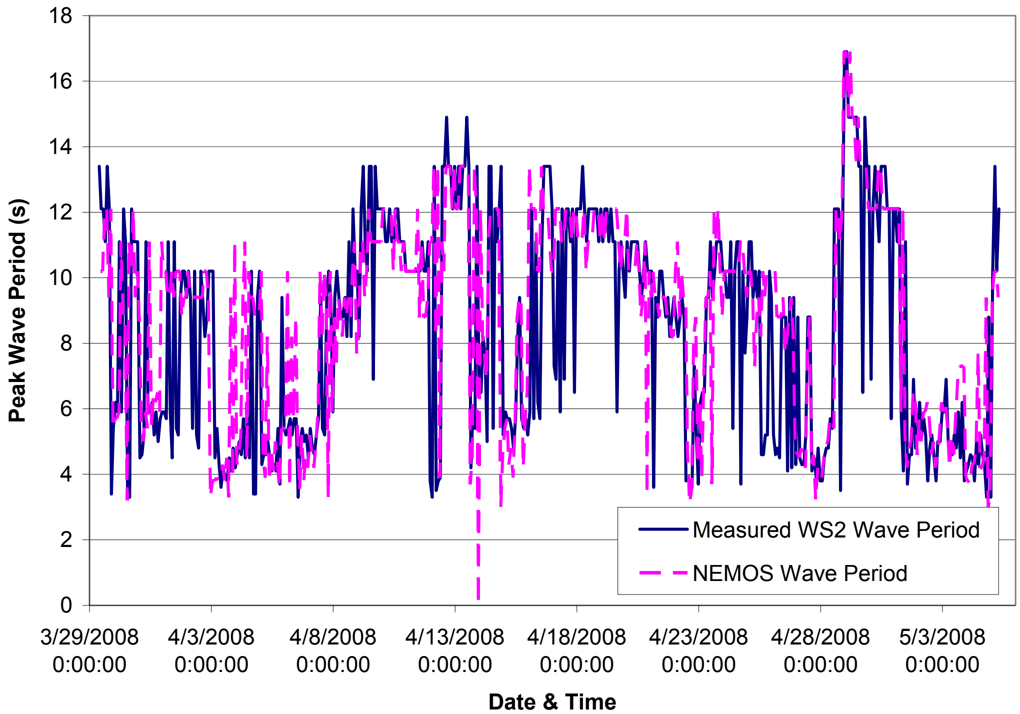

Figure 14: Comparison of Measured Wave Periods with WISPH3-Transformed Wave Periods at WS2

Utilizing the calibrated MIKE 21 Coupled Model FM, the model verification run applied the August 18 – 24, 2008 measured water surface elevations at WS1 and T2 to describe the model's offshore and north ICWW water level conditions. It also applied wave parameters measured over the same period at WS1 to describe the model's offshore wave parameter conditions. Figure 15 shows a comparison of the measured and simulated water levels at WS2. Simulated water levels first underestimate, and then overestimate the measured water levels. Similar to the variations seen during water level calibration, these differences may also result from different settling rates of the ADP instruments used to measure the water levels. Because an approaching hurricane prompted the quick retrieval of the ADP's, surveying of the instrument at WS2 only occurred at installation. Therefore, the change in sensor elevation for both ADP's remains unknown for this verification period, but likely caused the variability in simulated water levels. Figures 16 and 17 show comparisons of the measured and simulated wave parameters at WS1 and WS2. In each figure, the top graphs show the significant wave heights and wave directions, and the bottom graphs show the peak and mean wave periods. These figures generally show the model simulated well the wave heights, directions, and peak periods at WS1 and WS2. As mentioned in the model calibration section, because the measured wave data include the effects of wind (not modeled in the study simulations), lower mean wave periods result in the measured data when compared to the modeled mean wave periods. Given the good agreement of the model results and measured data, this study considered the model well calibrated and verified.

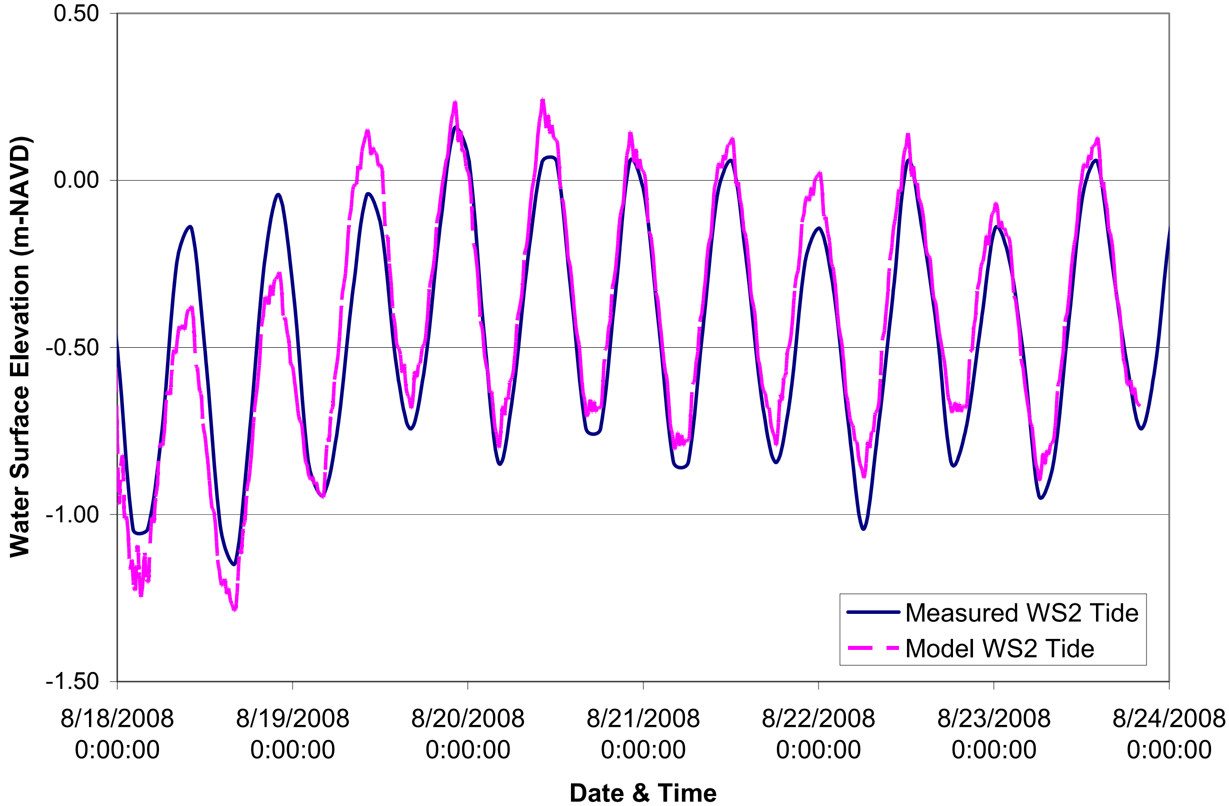

Figure 15: Comparison of Measured and Simulated Water Surface Elevations at WS2 during Verification

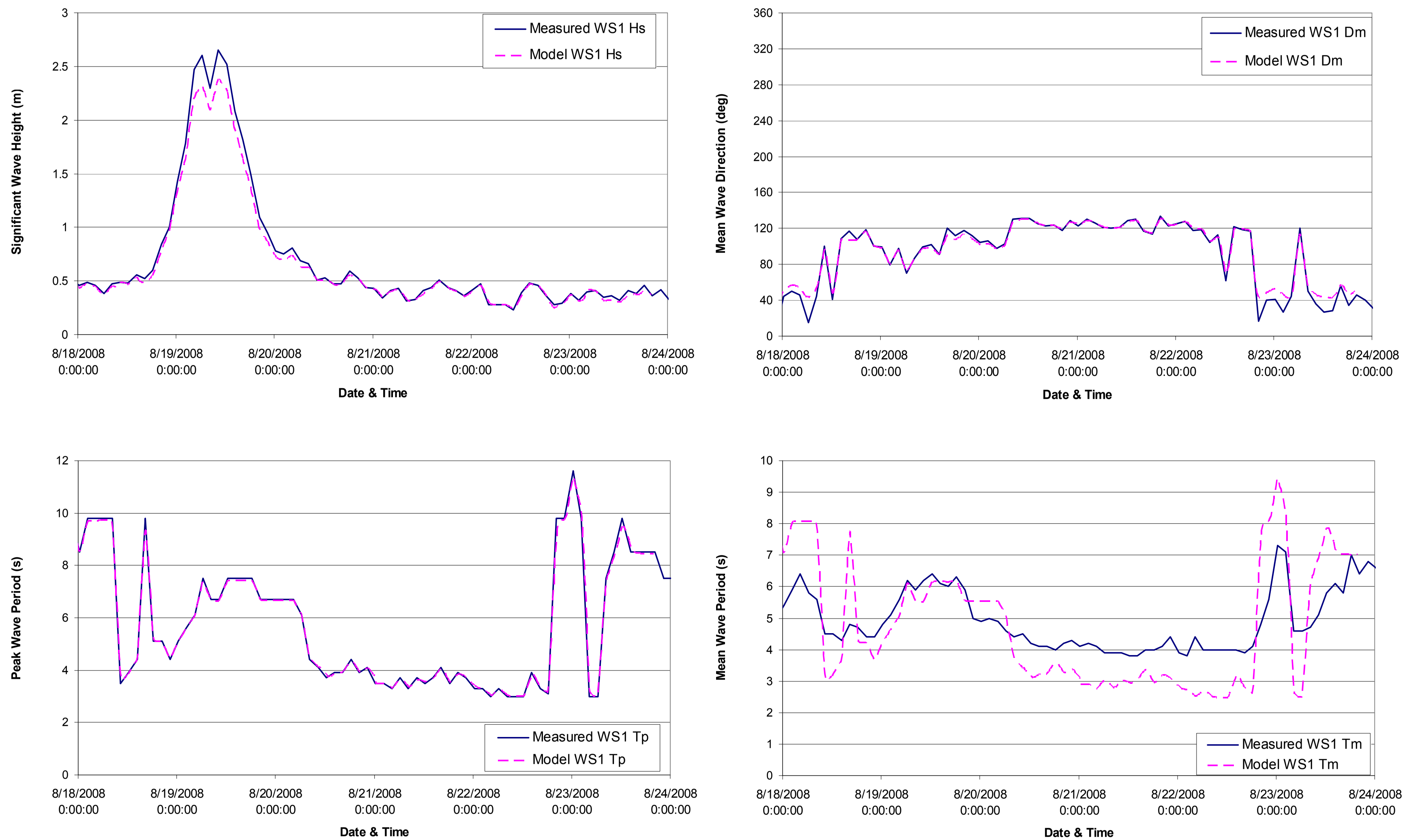

Figure 16: Comparison of Measured and Simulated Wave Parameters at WS1 during Verification

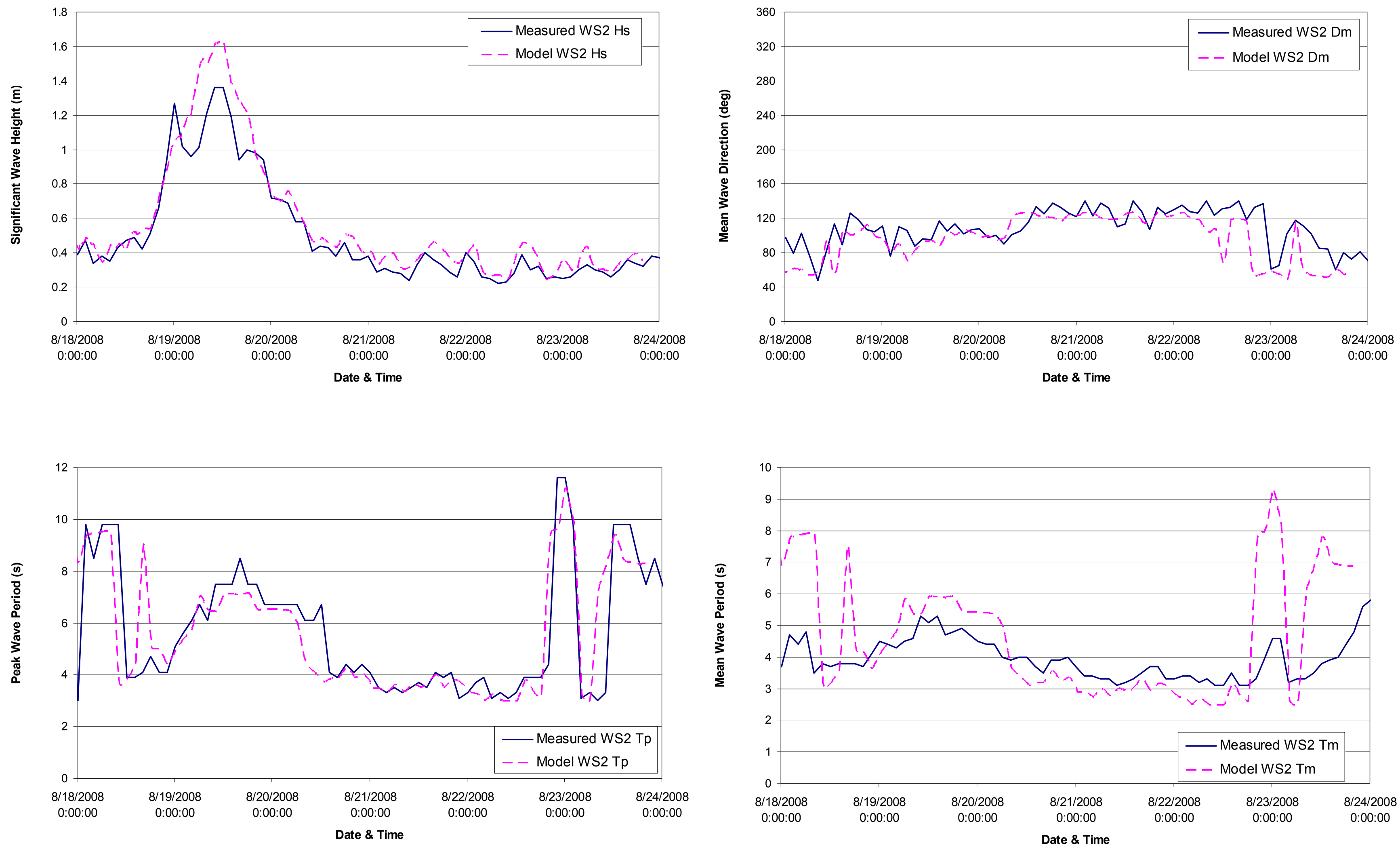

Figure 17: Comparison of Measured and Simulated Wave Parameters at WS2 during Verification

CONCLUSION

This study collected water surface elevation, current, wave, and wind data for two separate, approximately one month-long deployments: a one-month period in late winter/early spring and a one-month period in late summer. Each of these deployments captured a range of climatological conditions — including typical 'winter' conditions during the first data collection period and typical 'summer' (as well as tropical storm) conditions during the second data collection period. The measured water surface elevation, current, and wave data from these two collection periods, which likely bound the range of expected coastal conditions along the Jupiter/Carlin shoreline, allowed for the calibration and verification of site-specific hydrodynamic and wave models in a MIKE21 Coupled Model FM. The calibration and subsequent verification of the model provides the means for future assessment of the feasibility of stabilizing the Jupiter/Carlin shoreline with structural and non-structural alternatives.

REFERENCES

Kamphuis, J.W. 2000. Introduction to Coastal Engineering and Management. *Advanced Series on Ocean Engineering — Volume 16.* World Scientific Publishing Co. Pte. Ltd., Hackensack, NJ.

Palm Beach County Environmental Resources and Coastal Planning & Engineering, Inc. 1994. *Palm Beach County, Florida, From Martin County Line to Lake Worth Inlet and From South Lake Worth Inlet to Broward County Line, Shore Protection Project, General Design Memorandum Addendum for Jupiter/Carlin Segment, with Supplement to the Environmental Impact Statement,* West Palm Beach and Boca Raton, FL.